

16. Sauter D, Martin BJ, Di Renzo N, Vomscheid C. Analysis of eye tracking movements using innovations generated by a Kalman filter. *Med Biol Eng Comput.* 1991;29:63-69.
17. Bahill AT, Clark MR, Stark L. The main sequence, a tool for studying human eye movements. *Math Biosci.* 1975;24:191-204.
18. Williams CJ, Christian JC, Norton JA. TWINAN90: A Fortran program for conducting ANOVA-based and likelihood based analyses of twin data. *Comput Methods Programs Biomed.* 1992;38:167-176.
19. Christian JC, Kang KW, Norton JA. Choice of an estimate of genetic variance from twin data. *Am J Hum Genet.* 1974;26:154-161.
20. Iacono WG, Lykken DT. Two-year retest stability of eye tracking performance and a comparison of electro-oculographic and infrared recording techniques: evidence of EEG in the electro-oculogram. *Psychophysiology.* 1981;18:49-55.
21. Accardo AP, Pensiero S, Da Pozzo S, Perissuti P. Some characteristics of saccadic eye movements in children of primary school age. *Doc Ophthalmol.* 1992;80:189-199.

## In Vivo Demonstration of Increased Leukocyte Entrapment in Retinal Microcirculation of Diabetic Rats

Kazuaki Miyamoto,<sup>1</sup> Naoko Hiroshiba,<sup>1</sup>  
Akitaka Tsujikawa,<sup>1</sup> and Yuichiro Ogura<sup>2</sup>

**PURPOSE.** Leukocytes have been reported to be less deformable and more activated in diabetes. It has also been suggested that they cause microvascular occlusions that may cause diabetic microangiopathy. This study was designed to evaluate in vivo leukocyte dynamics in the retinal microcirculation of diabetic rats.

**METHODS.** Streptozotocin (STZ)-induced diabetic rats 4 weeks after diabetes induction and spontaneously diabetic Otsuka Long-Evans Tokushima Fatty (OLETF) rats with 6 weeks' duration of diabetes were used in this study. Leukocyte dynamics were observed with acridine orange digital fluorography, using a nuclear fluorescent dye of acridine orange and high-resolution images from a scanning laser ophthalmoscope.

**RESULTS.** There was no significant difference in capillary leukocyte velocity between the STZ-induced diabetic rats ( $1.27 \pm 0.12$  mm/sec, mean  $\pm$  SD) and nondiabetic control subjects ( $1.38 \pm 0.07$  mm/sec) or between OLETF rats ( $1.31 \pm 0.17$  mm/sec) and the nondiabetic controls, Long-Evans Tokushima Otsuka (LETO) rats ( $1.29 \pm 0.11$  mm/sec). In contrast, the density of leukocytes trapped in the retinal microcirculation was significantly elevated in the STZ-induced diabetic (2.5-fold;  $P < 0.01$ ) and the OLETF rats (2-fold;  $P < 0.01$ ) compared with leukocyte density in the control subjects.

**CONCLUSIONS.** Pharmacologically induced and spontaneously diabetic rats showed increased leukocyte entrap-

ment in the living retina in the early stages of diabetes. In light of the damaging potential of leukocytes, accumulation of leukocytes in diabetic retinas from the preretinopathy stage could cause microvascular occlusions and dysfunction, in turn causing diabetic retinopathy. (*Invest Ophthalmol Vis Sci.* 1998;39:2190-2194)

Capillary obstruction plays an important role as the initiator of the pathogenesis of diabetic retinopathy. Although capillary occlusions, subsequent vascular nonperfusion, and endothelial cell loss in early diabetic retinopathy are well understood clinically and histopathologically, little is known about the causes of the initial capillary occlusion.

In diabetes, leukocytes have been found to be less deformable<sup>1</sup> and more activated.<sup>2</sup> We have also studied the flow behavior of blood cells through microchannels that simulate capillaries and have reported that diabetic leukocytes occasionally plug the microchannels, prolonging the transit time of whole blood.<sup>3</sup> In addition, lower perfusion in the retina has been shown in the early stages of diabetes.<sup>4-6</sup> Thus, leukocytes can become trapped more easily in the retinal capillary bed of diabetes. Recent histopathologic studies have shown increased capillary occlusion and damage by leukocytes in the retina of diabetic rats<sup>2</sup> and in the choroid of patients with diabetes.<sup>7</sup> However, it is difficult to assess in vivo dynamic behavior of leukocytes in the microcirculation from histologic sections. Although an in vivo study recently showed that the incidence of leukocyte plugging increases throughout capillary networks in the skeletal muscle of diabetic rats,<sup>8</sup> no attempts have been made to examine leukocyte dynamics directly in the living retina.

We have recently developed a method called acridine orange digital fluorography that allows us to visualize leukocytes and examine leukocyte dynamics in rat retinal circulation in vivo.<sup>9,10</sup> In the present study, using this method, we investigated the dynamic behavior of leukocytes in the retinal microcirculation of streptozotocin (STZ)-induced diabetic rats, a chemically induced insulin-dependent diabetes mellitus model, and Otsuka Long-Evans Tokushima Fatty (OLETF) rats, a spontaneous model of non-insulin-dependent diabetes mellitus.

## METHODS

### Animals

All animals were managed in accordance with the ARVO Statement for the Use of Animals in Ophthalmic and Vision Research. For chemically induced diabetes, a rat model was used in which diabetes was induced by streptozotocin (STZ; Sigma Chemical, St. Louis, MO). Diabetes was induced in 5 Long-Evans rats, weighing

From the <sup>1</sup>Department of Ophthalmology and Visual Sciences, Kyoto University Graduate School of Medicine, Japan; and <sup>2</sup>Department of Ophthalmology, Nagoya City University Medical School, Japan.

Present address: <sup>1</sup>Surgical Research Laboratory, Enders 1013, Children's Hospital, 300 Longwood Avenue, Boston, MA 02115.

Submitted for publication February 24, 1998; revised June 5, 1998; accepted June 19, 1998.

Proprietary interest category: N.

Reprint requests: Yuichiro Ogura, Department of Ophthalmology, Nagoya City University Medical School, Mizuho-ku, Nagoya 467-8601, Japan.

approximately 200 g each, by intravenous injection of 60 mg/kg of STZ in physiologic saline. We confirmed that the plasma glucose level in each rat was greater than 13.9 mM 48 hours later. Five Long-Evans rats that were injected with an equal volume of saline alone served as nondiabetic control subjects. All rats were allowed free access to water and food for 4 weeks before acridine orange fluorography.

For the spontaneous diabetes model, Otsuka Long-Evans Tokushima Fatty (OLETF) rats were used. This model was developed by repeated selective bleeding of Long-Evans rats with hyperglycemia, mild obesity, and glycosuria.<sup>11</sup> The OLETF rat shows hyperglycemic obesity with hyperinsulinemia and insulin resistance similar to that of human non-insulin-dependent diabetes mellitus. Diabetic complications were reported, such as diffuse glomerulosclerosis and nodular lesions in the kidney, perivascular fibrosis in the heart, or thickened basement membranes of pericytes and deficient organelles in endothelial cells in the retinal capillaries. Long-Evans Tokushima Otsuka (LETO) rats that originated from the same colony of Long-Evans rats were established as the genetic control for OLETF rats. Four OLETF rats and four LETO rats were donated by Tokushima Research Institute (Otsuka Pharmaceutical, Tokushima, Japan). We verified that the fed plasma glucose level of OLETF rats became significantly higher than that of LETO rats from 18 weeks of age, as described in previous studies. Thus, we determined that the onset of diabetes in OLETF rats was at 18 weeks of age. The leukocyte dynamics in retinal microcirculation were studied in OLETF rats with 6 weeks' duration of diabetes when the average plasma glucose level exceeded 16.7 mM and reached the same level as that of STZ-induced diabetic rats and age-matched LETO rats.

### Acridine Orange Digital Fluorography

Leukocyte dynamics in the retina were observed using acridine orange digital fluorography. This technique in rats has been described previously.<sup>9,10</sup> Briefly, leukocytes were labeled with a fluorescent nuclear dye of acridine orange (Wako Pure Chemical, Osaka, Japan) administered intravenously and then imaged with a scanning laser ophthalmoscope (Rodentstock Instrument, Munich, Germany). The argon blue laser was used for the illumination source, with a regular emission filter for fluorescein angiography, because the spectral properties of leukocytes stained with acridine orange are similar to those of sodium fluorescein.

Immediately before acridine orange digital fluorography, rats were anesthetized with a 1:1 mixture of 4 mg/kg xylazine hydrochloride and 10 mg/kg ketamine hydrochloride, and the pupils were dilated with 0.5% tropicamide and 2.5% phenylephrine hydrochloride. Each rat had a catheter placed into the tail vein. The rat was then positioned on a movable platform according to the height of the chin rest of the scanning laser ophthalmoscope, and a focused image of the peripapillary fundus of the right eye was obtained. Acridine orange was dissolved in sterile saline at a concentration of 1.0 mg/ml, and the solution was injected through the tail vein catheter at a rate of 1 ml/min. The total dosage of dye was 5 mg/kg. The fundus was observed with the scanning laser ophthalmoscope in the 40° field for 3 minutes. Thirty minutes after the injection, the fundus was observed again to evaluate leukocyte entrapment in the retina. The obtained images were recorded on an S-VHS videotape at the rate of 30 frames/sec. After the experiment, the rat was killed with an anesthetic overdose, and the eye was

enucleated to determine a calibration factor for converting values measured on a computer monitor (in pixels) into real values (in micrometers). The calibration factor is the ratio between the actual size of each optic disc measured by microscopy and the apparent value on a computer monitor.

### Video Image Analysis

The video recordings were analyzed with an image analysis system, which has been described in detail elsewhere.<sup>9,10</sup> The system consists of a computer equipped with a video digitizer (Radius, San Jose, CA) that digitizes the video image in real time (30 frames/sec) to 640 × 480 pixels with an intensity resolution of 256 steps. Using this system, the flow velocity of leukocytes in retinal capillaries and the density of leukocytes trapped in the retina were determined.

The leukocyte velocity in capillaries was measured with frame-by-frame analysis of the cell position. The digitized images were processed by subtracting each frame from the previous one. The center position of each leukocyte in the generated image was marked on a computer monitor, and the distance between the marked positions was measured in pixels as a straight line. The time interval between two marked positions corresponded to the duration of one video frame, or 33.3 msec. The capillary velocity of one leukocyte was determined by averaging the velocities measured in at least five consecutive frames. The average of 40 to 50 velocities in at least 15 capillaries was used as the capillary leukocyte velocity for each rat.

Leukocyte entrapment in retinal microcirculation was evaluated in video images recorded 30 minutes after acridine orange injection, as described previously.<sup>10</sup> Briefly, an observation area surrounding the optic disc was determined by drawing a polygon surrounded by the adjacent major retinal vessels. The area was measured in pixels on a computer monitor, and the density of trapped leukocytes was calculated by dividing the number of trapped leukocytes that were recognized as fluorescent dots by the area of the observation region. The densities of leukocytes were calculated generally in eight peripapillary observation areas. An average density of trapped leukocytes for each rat was obtained by averaging the eight density values. All data were converted into real values, by using the calibration factor described earlier.

### Leukocyte Count in Peripheral Blood

Blood anticoagulated with EDTA was drawn from the abdominal aorta of each rat after the experiment. The blood sample was analyzed using a hematology analyzer (Coulter Counter T-890; Coulter Electronics, Tokyo, Japan).

### Statistical Analysis

Results are expressed as mean ± SD. Statistical analyses were performed using a two-sample *t*-test or a two-sample *t*-test with Welch's correction. *P* < 0.05 was considered statistically significant.

## RESULTS

### Characteristics of Diabetic Rats and Control Subjects

The comparison between the diabetic rats and the control subjects in body weight, fed plasma glucose, mean blood

TABLE 1. Characteristics of Diabetic Rats and Control Subjects

	STZ	Control	<i>P</i> *	OLETF	LETO	<i>P</i> *
Body weight (g)	289 ± 27	344 ± 23	0.008	584 ± 17	491 ± 17	0.0002
Plasma glucose (mM)	20.6 ± 3.3	6.7 ± 1.7	0.00003	17.6 ± 2.5	8.8 ± 1.6	0.001
Blood pressure (mm Hg)	102 ± 12	114 ± 16	NS	117 ± 15	110 ± 9	NS
Leukocyte count (×10 <sup>3</sup> /μl)	6.2 ± 1.7	6.4 ± 1.5	NS	4.3 ± 0.9	4.9 ± 0.4	NS

STZ, streptozotocin-induced diabetic rats; OLETF, Otsuka Long-Evans Tokushima Fatty rats; LETO, Long-Evans Tokushima Otsuka rats; NS, not significant.

Values are means ± SD.

\* Comparison between control and diabetic rats (two-sample *t*-test).

pressure, and leukocyte count in peripheral blood is shown in Table 1. In body weight, STZ-induced diabetic rats had significantly lower weights ( $P = 0.008$ ) than control rats, and OLETF rats had significantly higher weights ( $P = 0.0002$ ) than LETO rats. The plasma glucose levels of STZ-induced diabetic and OLETF rats were significantly higher ( $P = 0.00003$  and  $P = 0.001$ , respectively) than those of the control subjects. There were no significant differences in mean blood pressure and leukocyte count in peripheral blood between the diabetic and control rats.

#### Leukocyte Dynamics in Retinal Capillary Bed

Leukocytes flowed through the retinal capillaries at a fairly constant speed without stopping, in diabetic and control rats. In either STZ-induced diabetic or OLETF rats, no leukocytes were observed plugging the capillaries in even one video frame, at least during the observation period, or for 3 minutes after the beginning of acridine orange injection. Leukocyte velocities in capillaries were  $1.27 \pm 0.12$  mm/sec in the STZ-induced diabetic rat group and  $1.38 \pm 0.07$  mm/sec in the control group. There was no significant difference between the two groups, although the capillary leukocyte velocity of STZ-induced diabetic rats tended to be lower than that of the control subjects ( $P = 0.09$ ). There was also no significant difference in capillary leukocyte velocity between OLETF rats ( $1.31 \pm 0.17$  mm/sec) and LETO rats ( $1.29 \pm 0.11$  mm/sec).

#### Leukocyte Entrapment in Retinal Microcirculation

The dye of acridine orange quickly stains circulating leukocytes and vascular endothelial cells and then diffuses into the

retina through blood vessel walls because of its membrane permeability. After the dye injection ended, the fluorescence of the retina and circulating leukocytes decreased gradually, owing to the washout effect. In contrast, because leukocytes trapped in the retinal microcirculation remain fluorescent for a longer period,<sup>10</sup> they became more distinguishable 30 minutes after acridine orange injection, when the number of trapped leukocytes was counted. Digitized images of the ocular fundus obtained from an STZ-induced diabetic rat and a control rat 30 minutes after dye administration are shown in Figure 1. The trapped leukocytes, recognized as fluorescent dots, were observed more in the STZ-induced diabetic group than in the control group. Similarly, OLETF rats showed more leukocyte entrapment than LETO rats. The density of trapped leukocytes in STZ-induced diabetic rats was  $10.1 \pm 3.6$  cells/mm<sup>2</sup>, which was significantly elevated ( $P = 0.008$ ) compared with that in control subjects ( $4.1 \pm 1.4$  cells/mm<sup>2</sup>; Fig. 2A). The OLETF rats also showed a significant increase in the density of trapped leukocytes ( $12.0 \pm 2.8$  cells/mm<sup>2</sup>,  $P = 0.008$ ) compared with LETO rats ( $6.0 \pm 1.2$  cells/mm<sup>2</sup>; Fig. 2B).

#### DISCUSSION

The present study shows that entrapment of leukocytes is significantly increased in the retinal microcirculation not only of chemically induced diabetic rats but also of spontaneously diabetic rats. Recent histopathologic studies showed many capillaries occluded by leukocytes in retinas of chemically induced diabetic rats<sup>2</sup> and increased numbers of polymorpho-

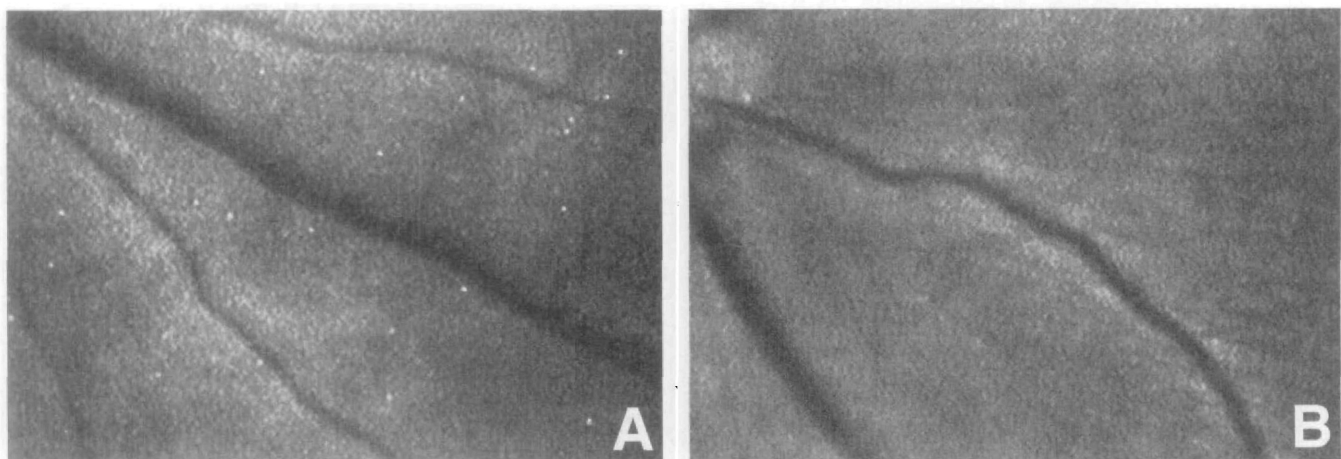


FIGURE 1. Digitized images of ocular fundus obtained from a streptozotocin (STZ)-induced diabetic rat (A) and a control (B) 30 minutes after acridine orange injection. The trapped leukocytes are recognized as fluorescent dots.

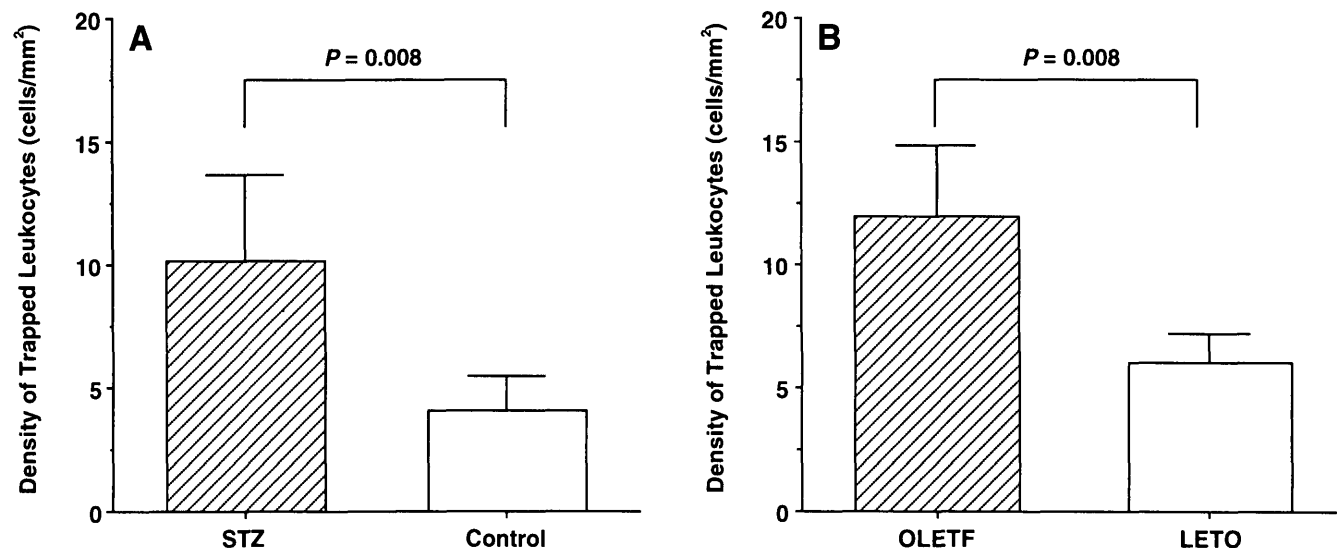


FIGURE 2. Density of leukocytes trapped in the retinal microcirculation. (A) Streptozotocin (STZ)-induced diabetic rats and control subjects. (B) Otsuka Long-Evans Tokushima Fatty (OLETF) and Long-Evans Tokushima Otsuka (LETO) rats. Values are means  $\pm$  SD.

nuclear leukocytes in retinas of patients with diabetes.<sup>12</sup> In the retinas of living diabetic rats, we could provide the first direct evidence in agreement with the previous histologic observations. In one study of leukocyte behavior in diabetic microcirculation other than the eye, Harris et al.<sup>8</sup> reported that the incidence of leukocyte plugging was increased in the skeletal muscles of STZ-induced diabetic rats, resulting in a significant increase in capillary network resistance. Our result is also consistent with their findings.

Two major reasons could be considered for increased leukocyte entrapment in the diabetic retina: One is alterations of leukocyte properties and the other, alterations of the microvasculature itself. In diabetes, various changes in the properties of leukocytes have been reported. First, many filtration studies have shown that diabetic leukocytes are less filterable, that is, less deformable than normal leukocytes. In addition, decreased fluidity of the leukocyte membrane was described in STZ-induced diabetic rats. Second, leukocytes have been reported to be more activated in diabetes. The activation would make leukocytes more rigid because of increased polymerization and network organization of F-actin microfilaments, resulting in increased entrapment of leukocytes in the microvasculature. In fact, chemically activated leukocytes were shown to plug the capillaries and increase microvascular resistance. Third, leukocyte adhesion energy to the vascular endothelium is elevated in the diabetic environment. Recent *in vitro* studies have shown that neutrophils, after hyperglycemic treatment, exhibited increased adhesion to retinal endothelial cells.<sup>13</sup> *In vivo* data also show increased monocyte adhesion to the endothelium in alloxan-induced diabetes. Moreover, monocytes from patients with diabetes have increased surface expression of the adhesion molecule CD11b-CD18 and show greater adhesion to endothelial cells.<sup>14</sup> These alterations of leukocyte properties in diabetes could cause enhanced entrapment in the microcirculation.

In addition, changes in the microvasculature can cause an increased number of trapped leukocytes. It has been reported in patients with diabetes with no retinopathy, that is, in the early stages of diabetes, that blood speed in retinal arteries is

significantly lower<sup>4</sup> and retinal blood flow is significantly decreased<sup>5</sup>; moreover, reduced retinal blood flow was also recorded in rats with STZ-induced diabetes of short duration,<sup>6</sup> the same type of rats that were used as an insulin-dependent diabetes mellitus model in our study. Under conditions of low perfusion, leukocytes could become trapped mechanically in the capillaries. Also, there is a possibility that vasoconstriction at the microvascular level may occur in the early stages of diabetes through increased expression of endothelin-1<sup>15</sup> or elevated protein kinase C activity.<sup>6</sup> Protein kinase C has been shown to promote vasoconstriction and to be increased in the retinas of rats with STZ-induced diabetes of short duration. A decrease in capillary diameter has been observed in the early stages of diabetes of STZ-induced diabetic rats.<sup>8</sup> An additional possibility is that leukocyte entrapment may be mediated by adhesion molecules, such as intercellular adhesion molecule-1 and vascular cell adhesion molecule-1. High glucose treatment significantly increases intercellular adhesion molecule-1 surface expression in cultured endothelial cells.<sup>16</sup> Furthermore, increased intercellular adhesion molecule-1 immunoreactivity has been observed in the retinal vascular endothelium of patients with diabetes.<sup>12</sup> It remains to be studied whether the expression of adhesion molecules are elevated in the early stages of diabetic rats.

In the present study, no significant change was observed in capillary leukocyte velocity between diabetic animals and their control subjects. This may seem somewhat anomalous if leukocytes are prone to becoming trapped in the microcirculation. However, when leukocytes enter microvascular bifurcations, they preferentially flow into the pathway with higher flow rate. We also showed a similar preferential distribution of leukocytes in the retinal microcirculation.<sup>9</sup> If this shunting effect of leukocytes is preserved, no change in leukocyte flow velocity in capillaries would be expected.

Leukocyte entrapment in the diabetic retina may play an important role in the stage before observable retinopathy develops, because leukocytes trapped in the capillaries may cause flow disturbances and the capillary nonperfusion that follows, which is the hallmark of early diabetic retinopathy.

Moreover, entrapped leukocytes could increase vascular permeability by damaging the blood-retinal barrier. Furthermore, once leukocytes interact strongly with the vascular endothelium, they may initiate endothelial dysfunction and damage by releasing oxygen-derived free radicals and proteolytic enzymes. Diabetic leukocytes have been reported to produce more superoxide radicals than normal leukocytes. Recent histologic studies showed the presence of leukocytes to be associated with increased vascular endothelial cell injury and subsequent vascular occlusion in the rat diabetic retina<sup>2</sup> and in the human diabetic choroid.<sup>7</sup> Therefore, the increased leukocyte entrapment in the diabetic retina may act as an initiator in a chain of events leading to diabetic retinopathy.

## References

1. Vermes I, Steinmetz ET, Zeyen LJ, van-der-Veen EA. Rheological properties of white blood cells are changed in diabetic patients with microvascular complications. *Diabetologia*. 1987;30:434-436.
2. Schröder S, Palinski W, Schmid-Schönbein GW. Activated monocytes and granulocytes, capillary nonperfusion, and neovascularization in diabetic retinopathy. *Am J Pathol*. 1991;139:81-100.
3. Miyamoto K, Ogura Y, Kenmochi S, Honda Y. Role of leukocytes in diabetic microcirculatory disturbances. *Microvasc Res*. 1997;54:43-48.
4. Fekete GT, Buzney SM, Ogasawara H, et al. Retinal circulatory abnormalities in type 1 diabetes. *Invest Ophthalmol Vis Sci*. 1994;35:2968-2975.
5. Bursell SE, Clermont AC, Kinsley BT, Simonson DC, Aiello LM, Wolpert HA. Retinal blood flow changes in patients with insulin-dependent diabetes mellitus and no diabetic retinopathy. A video fluorescein angiography study. *Invest Ophthalmol Vis Sci*. 1996;37:886-897.
6. Bursell SE, Takagi C, Clermont AC, et al. Specific retinal diacylglycerol and protein kinase C beta isoform modulation mimics abnormal retinal hemodynamics in diabetic rats. *Invest Ophthalmol Vis Sci*. 1997;38:2711-2720.
7. Luty GA, Cao J, McLeod DS. Relationship of polymorphonuclear leukocytes to capillary dropout in the human diabetic choroid. *Am J Pathol*. 1997;151:707-714.
8. Harris AG, Skalak TC, Hatchell DL. Leukocyte-capillary plugging and network resistance are increased in skeletal muscle of rats with streptozotocin-induced hyperglycemia. *Int J Microcirc*. 1994;14:159-166.
9. Nishiwaki H, Ogura Y, Kimura H, Kiryu J, Miyamoto K, Matsuda N. Visualization and quantitative analysis of leukocyte dynamics in retinal microcirculation of rats. *Invest Ophthalmol Vis Sci*. 1996;37:1341-1347.
10. Nishiwaki H, Ogura Y, Miyamoto K, Matsuda N, Honda Y. Interferon alpha induces leukocyte capillary trapping in rat retinal microcirculation. *Arch Ophthalmol*. 1996;114:726-730.
11. Kawano K, Hirashima T, Mori S, Saitoh Y, Kurosumi M, Natori T. Spontaneous long-term hyperglycemic rat with diabetic complications. Otsuka Long-Evans Tokushima Fatty (OLETF) strain. *Diabetes*. 1992;41:1422-1428.
12. McLeod DS, Lefer DJ, Merges C, Luty GA. Enhanced expression of intracellular adhesion molecule-1 and P-selectin in the diabetic human retina and choroid. *Am J Pathol*. 1995;147:642-653.
13. Bullard SR, Hatchell DL, Cohen HJ, Rao KM. Increased adhesion of neutrophils to retinal vascular endothelial cells exposed to hyperosmolarity. *Exp Eye Res*. 1994;58:641-647.
14. Dosquet C, Weill D, Wautier JL. Molecular mechanism of blood monocyte adhesion to vascular endothelial cells. *Nouv Rev Fr Hematol*. 1992;34(suppl):S55-S59.
15. Takahashi K, Brooks RA, Kanse SM, Ghatei MA, Kohner EM, Bloom SR. Production of endothelin 1 by cultured bovine retinal endothelial cells and presence of endothelin receptors on associated pericytes. *Diabetes*. 1989;38:1200-1202.
16. Baumgartner-Parzer SM, Wagner L, Pettermann M, Gessl A, Waldhausl W. Modulation by high glucose of adhesion molecule expression in cultured endothelial cells. *Diabetologia*. 1995;38:1367-1370.

## Matrix Metalloproteinases and Metalloproteinase Inhibitors in Choroidal Neovascular Membranes

Björn Steen,<sup>1,2</sup> Sylvia Sejersen,<sup>1,2</sup>  
Lennart Berglin,<sup>1</sup> Stefan Seregard,<sup>1</sup> and  
Anders Kvanta<sup>1,2</sup>

**PURPOSE.** Matrix metalloproteinases (MMP) are a family of extracellular matrix degrading enzymes associated with the development of neovascularization. To investigate the

possible role of these enzymes in choroidal neovascularization, the mRNA expression of MMPs and tissue inhibitors of metalloproteinases (TIMPs) were analyzed in subfoveal fibrovascular membranes from patients with age-related macular degeneration (AMD).

**METHODS.** Surgically removed subfoveal fibrovascular membranes from five eyes were analyzed for the expression of MMP and TIMP mRNA. In situ hybridization antisense and sense riboprobes were generated using DNA complementary to human collagenase (MMP-1), 72 kDa gelatinase (MMP-2), stromelysin (MMP-3), 92-kDa gelatinase (MMP-9), TIMP-1, TIMP-2, and TIMP-3. Vascular endothelial cells were detected using immunostaining for von Willebrand factor.

**RESULTS.** MMP-2 and MMP-9 mRNA were detected in all specimens. Most of the membranes also expressed TIMP-1 and TIMP-3 mRNA, and two of the membranes expressed TIMP-2 mRNA. MMP-2, TIMP-1, and TIMP-2 mRNA had a similar overall distribution that was relatively uniform within the vascularized membrane stroma. MMP-2 expression appeared to be localized mainly to the vascular endothelial cells, whereas TIMP-1 and TIMP-3 were detected in other cell types such as fibroblastlike cells. MMP-9 expression was distinctly

From the <sup>1</sup>Department of Ophthalmology, St. Erik's Eye Hospital, and the <sup>2</sup>Department of Physiology and Pharmacology, Karolinska Institute, Stockholm, Sweden.

Supported by grants from The Margit Thyselius Foundation, The Kronprinsessan Margaretas Foundation, and The Edwin Jordan Foundation, Stockholm, Sweden.

Submitted for publication February 4, 1998; revised June 4, 1998; accepted June 19, 1998.

Proprietary interest category: N.

Reprint requests: Anders Kvanta, St. Erik's Eye Hospital, Karolinska Institute, Polhemsgatan 50, SE-112 82 Stockholm, Sweden.